Determination of Isomeric Dibenzo[*a*,*l*]pyrene-Adenine Adducts by Six Different Tandem Mass Spectrometric Experiments

Jaeman Byun, Jonathon Gooden, and Ragulan Ramanathan
Department of Chemistry, Washington University, St. Louis, Missouri, USA

Kai-Ming Li and Ercole L. Cavalieri
Eppley Institute for Research in Cancer and Allied Diseases, University of Nebraska Medical Center, Omaha, Nebraska, USA

Michael L. Gross
Department of Chemistry, Washington University, St. Louis, Missouri, USA

Six different tandem-mass-spectrometric experiments were evaluated to assess their ability to distinguish four isomeric, carcinogen-modified adenines. Metastable-ion dissociations and high-energy collisional activated decompositions (HE CAD) of fast-atom bombardment (FAB)-produced ions were followed on a four-sector tandem mass spectrometer. Precursor ions were also produced by electrospray on the four-sector instrument, and they were submitted to both high-energy and electrospray ionization (ESI)-source CAD. We contrasted these means of activation with low-energy (LE) CAD of electrospray-produced ions on a triple quadrupole instrument and with post-source decompositions (PSD) of ions produced by matrix-assisted laser desorption ionization (MALDI). The latter experiment was conducted with a time-of-flight mass spectrometer. The four subject molecules were isomeric dibenzo-[*a*,*l*]pyrene (DB[*a*,*l*]P) adenine adducts, in which *N*1, *N*3, *N*7, and N^6 positions were substituted. We used similarity indicies (SI), which were calculated from the relative abundances of common fragment ions for the isomers, to confirm quantitatively that HE CAD of FAB and ESI-produced ions can distinguish two of three, and that LE CAD and MALDI-PSD can distinguish three of the three isomers that give qualitatively identical product-ion spectra. The results also show that LE CAD and MALDI-PSD have comparable discriminating capability for these three DBP adducts. (J Am Soc Mass Spectrom 1997, 8, 977–986) © 1997 American Society for Mass Spectrometry

The first critical event in the carcinogenesis of polycyclic-aromatic-hydrocarbons (PAH) is the chemical reaction of dibenzo[*a*,*l*]pyrene (DB[*a*,*l*]P), benzo[*a*]pyrene (BP), dimethylbenz[*a*]anthracene (DMBA), and other PAH with DNA [1–4]. The PAH are metabolically activated by at least one of two known pathways: one-electron oxidation to yield reactive intermediate radical cations [5–7] or multielectron oxidation to generate bay-region diol epoxides [8, 9]. Because metabolic activation is not site-directed, positional isomers are produced in the radical-cation reaction and, in addition, stereo isomers in the diol-epoxide reactions. One must be able to differentiate these isomeric adducts to understand the metabolic pathways of activation and the role of modified DNA in tumor initiation.

Address reprint requests to Dr. M. L. Gross, Department of Chemistry, Washington University, St. Louis, MO 63130. E-mail: mgross@wuchem.wustl.edu

A major analytical challenge is the characterization of adducts produced by xenobiotics reacting to modify DNA in vitro and in vivo. Fluorescence spectroscopy [10, 11], ^{32}P-postlabeling [12, 13], and immunoassay [14, 15], which are commonly used for characterizing these adducts at physiologically important levels, provide little structural information. Previously, we showed that fast-atom bombardment (FAB) combined with tandem mass spectrometry is effective for distinguishing and characterizing BP-, DB[*a*,*l*]P-, and DMBA-DNA adducts that were prepared as reference compounds or isolated from in vitro experiments [16–18].

In this article, we extend those studies and describe the use of six different tandem-mass-spectrometric experiments to determine a unique set of adenine (ade) modified by dibenz[*a*,*l*]pyrene (DB[*a*,*l*]P). We chose these isomeric adducts to serve as appropriate and challenging models for comparing (1) metastable-ion and (2) high-energy collisional activated decompositions (HE CAD) of FAB-produced ions, (3) electrospray

1044-0305/97/$17.00
PII S1044-0305(97)00125-6

Received March 20, 1997
Revised May 16, 1997
Accepted May 19, 1997

ionization (ESI)-source CAD and (4) HE CAD of ESI-produced ions, (5) low-energy (LE) CAD, and (6) post-source decompositions (PSD). LE CAD spectra were obtained with three different triple quadrupole mass spectrometers. PSD was studied for matrix-assisted laser desorption ionization (MALDI)-produced ions in a time-of-flight (TOF) mass spectrometer [19]. Although the metastable-ion (MI) decompositions are not commonly used for structure determination, this method does reveal the lowest-energy fragmentations for a given ionization method and assists us with understanding the underlying fragmentation chemistry of modified adenine.

The ability to distinguish isomeric DNA adducts is expected to be a challenge for tandem mass spectrometry. To facilitate comparing one spectrum with another and for assessing the reproducibility of spectra, we reintroduce a statistical parameter called a similarity index (SI), which we advocated earlier for comparing structures of isomers in ion-chemistry studies [20].

These studies would not be possible and the prospects for understanding DNA modification would be slight were it not for the introduction of FAB, MALDI, and ESI. Workers in other laboratories are also taking advantages of these ionization methods coupled with tandem mass spectrometry to characterize carcinogen-DNA adducts [21–24]. Most reports are of method developments, and they set the stage for applications in biological studies. None of those reports, however, use a set of isomers to compare and contrast various tandem mass spectrometry experiments.

Experimental

Materials

The adducts were prepared at the Eppley Institute for Research in Cancer and Allied Diseases by using electrochemical oxidation of DB[*a*,*l*]P in the presence of adenine [25]. UV, NMR, exact-mass measurements, and tandem mass spectrometry (MS/MS) in the FAB ionization mode were used to establish the structures of the BP and DB[*a*,*l*]P-DNA adducts [17, 25–27].

Instrumentation

HE CAD spectra were obtained by using a VG-ZAB-T (Manchester, UK), a four-sector tandem mass spectrometer of BEBE design [28]. The first stage mass analyzer, MS1, is a high-resolving-power, double-focusing mass spectrometer (ZAB) of reverse geometry. The second stage, MS2, is a prototype Mattauch–Herzog-type design, incorporating a standard magnet and a planar electrostatic analyzer (ESA) of inhomogeneous electric field.

For FAB ionization, 10–15 nmol of sample was dissolved in 10 μL of MeOH or DMSO, and a 1-μL aliquot was loaded on the probe along with 1 μL of 1:1 3-nitrobenzyl alcohol and glycerol (3-NBA/GLY), which proved to give the best response compared to 3-NBA, GLY and 1% trifuroacetic acid (3-NBA/GLY/TFA), and GLY, DMSO, and 1% heptafluorobutyric acid (GLY/DMSO/HFBA). A Cs^+ ion gun operated at 30 keV was used to desorb the ions from the probe tip. The instrument accelerating voltage was +8.0 kV.

CAD mass spectra were obtained after precursor-ion activation in the third field-free region (between MS1 and MS2). Helium was added to the collision cell (floated at 4 kV) to attenuate the ion beam by 50%. MS1 was operated at a resolving power of 1000; the resolving power of MS2 was set to 1000 (full width at half-height definition). For high-energy CAD of the ESI-produced ions, the collision cell was floated at 2 kV, the amount of helium introduced into the collision cell was sufficient to attenuate the ion beam by 80%, and the resolving power of MS2 was approximately 500. Ten to fifteen 15-s scans were signal-averaged for each spectrum. No collision gas was used for metastable-ion experiments. Data acquisition and workup were carried out with a VG (Manchester, UK) data system equipped with a DEC Alpha 3000 workstation, OPUS V 3.1X software, and a VG SIOS I interface.

To obtain the best tandem mass spectra, it was necessary to tune MS2 by desorbing glycerol clusters and collisionally activating the m/z 461 ion. This allowed MS2 (magnet 2 and ESA 2) to be optimized for maximum transmission of product ions and a calibration file to be developed for mass measurement of product ions. Mass assignments of fragment ions in tandem mass spectra were achieved by using a location data file that was generated by recording the Hall-probe voltage in a manner that was similar to that used for MS1. In the MS/MS mode, this location data also served to define the necessary ESA scan program to achieve the correct B/E relationship for spectral scanning.

High-energy, tandem mass spectra of ESI-produced DB[*a*,*l*]P adducts and ESI-source CAD were also obtained by using the VG-ZAB-T and a VG ESI source. The ESI needle was held at 8000 V and the counter electrode ("pepper pot") at 5000 V. To induce CAD in the high-pressure region between the sampling cone and the skimmer, the sampling cone potential was increased to be approximately 160 V above the optimal operating potential of 4177 V. Skimmer lens, skimmer, ring electrode, and hexapole were typically held at 4125, 4119, 4117, and 4116 V, respectively. Nitrogen was used as bath and nebulizer gas with a flow rate of 400 and 12 L/h, respectively. Sufficient sample was dissolved in 33/33/33/1 methanol/water/acetonitrile/acetic acid to give a solution concentration of approximately 5 pmol/μL and injected into the flow of a similar solvent via a six-port Rheodyne 7125 injector with a 20-μL external loop. A Harvard model 22 syringe pump was used to infuse the solvent to the needle at a flow rate of 10 μL/min.

LE CAD experiments were carried out with a Finnigan TSQ 7000 (San Jose, CA), a Micromass Quattro II (Manchester, UK), and a Sciex API 300 triple quadru-

pole (Thornhill, Canada) mass spectrometers, which were equipped with ESI sources. The LE CAD mass spectra shown here for DB[*a*,*l*]P-Ade adducts were acquired on API 300 triple quadrupole mass spectrometry system. All samples were introduced as a solution of approximately 1 pmol/μL with an Ionspray source (Sciex) or electrospray sources typically at a flow rate of 5 μL/min (Sciex and Finnigan) or 2 μL/min (Micromass). The electrospray needle was held at 5000 V (Sciex) or 4000 V (Finnigan and Micromass) and the counterelectrode at ground potential. The solvent system of 33/33/33/1 methanol/water/acetonitrile/acetic acid was used to prepare the sample and served as a carrier solvent. For MS/MS experiments, argon (Finnigan) or nitrogen (Sciex and Micromass) was used at a pressure of approximately 10 mTorr. The collision energy was varied by changing the offset voltage of Q2 with respect to that of Q1 (the variation of the product-ion spectrum with collision energy was investigated systematically with the Sciex instrument). For comparison of product-ion spectra, a collision energy of 55 eV (offset of Q2 was 55 eV with respect to Q1) was chosen. Experiments performed on a Finnigan TSQ 7000 and a Micromass Quattro II triple quadrupole instrument were carried out under the same conditions as used on a Sciex API 300 triple quadrupole mass spectrometer. Ten 0.8-s scans (Sciex) were signal-averaged for each spectrum. Acquisitions for 20 s on a Finnigan TSQ 7000 and for 10 s on a Micromass instrument were signal-averaged for each spectrum, respectively.

The MALDI-TOF experiments were carried out on a PerSeptive Biosystems, Inc. Voyager RP (Cambridge, MA). A nitrogen laser (337-nm, 20-kW peak laser power, 2-ns pulse width) was used to desorb the sample ions. The instrument was operated in the reflectron mode with an accelerating potential of 25 kV. Post-source-decay (PSD) experiments [19b] were carried out under the same conditions. The synthesis of the MALDI matrix 4-benzyloxy-α-cyanocinnamic acid (BCC) was described elsewhere [29]. A solution of 0.25-M *d*-fucose in 1% TFA and 50% acetonitrile/water was saturated with BCC, mixed with the analyte in a 1:1 ratio on the sample plate to deposit 1–2 pmol of analyte, and allowed to air dry. MALDI-TOF spectra were from 40 to 60 laser pulses, whereas PSD spectra were from 50 to 200 laser pulses. Raw data were acquired with a Tektronix 520A digitizing oscilloscope before being transferred to a Micron 486 computer equipped with GRAMS/386 software (Galactic Industries).

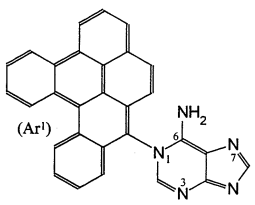

(I) Ar^1 = 1, DB[*a*,*l*]P-10-*N*1Ade
(II) Ar^1 = 3, DB[a,l]P-10-*N*3Ade
(III) Ar^1 = 7, DB[*a*,*l*]P-10-*N*7Ade
(IV) Ar^1 = 6, DB[*a*,*l*]P-10-*N*^{6}Ade

where Ar^1 = dibenzo[*a*,*l*]pyrenyl

Results and Discussion

We used six tandem-mass-spectrometric experiments to investigate the structural isomers of four DB[*a*,*l*]P-Ade adducts (see structures **I–IV**): one with the C-10 of the DB[*a*,*l*]P bound to the N^6 of the exocyclic nitrogen and three others, with DB[*a*,*l*]P bonded at *N*-1, *N*-3, and *N*-7 of the ring system of the adenine moiety, respectively. In the first and second experiments, we produced $[M + H]^+$ ions by FAB ionization, and allowed the mass-selected ions to undergo MI dissociations and HE CAD on a four-sector tandem mass spectrometer. We also used the same instrument, but prepared the ions by ESI and activated them by ESI-source CAD and high-energy collisions. We chose also to prepare the ions by ESI and to activate them by low-energy collisions on three different triple quadrupole instruments. In the sixth experiment, we generated the $[M + H]^+$ ions by MALDI and allowed them to undergo post-source dissociations in a TOF mass spectrometer equipped with a reflectron.

CAD of DB[a,l]P-Adenine Adducts

FAB of the four DB[*a*,*l*]P-Ade adducts when the matrix was 3-nitrobenzyl alcohol/glycerol produced an $[M + H]^+$ of *m*/*z* 436. This matrix system gave the best sample ion current compared to those produced with 3-NBA, GLY, 3-NBA/GLY/TFA, and GLY/TFA. The exact masses of these adducts, as determined by high-resolution peak matching, were within 1.0 ppm of the theoretical value for $C_{29}H_{18}N_5$. We then investigated these four nitrogen-substituted isomers to judge the effectiveness of various forms of tandem mass spectrometry to distinguish positional isomers of modified adenine.

Under HE CAD conditions, the $[M + H]^+$ ions of DB[*a*,*l*]P-10-*N*1Ade (**I**), DB[*a*,*l*]P-10-*N*3Ade (**II**), and DB[*a*,*l*]P-10-*N*7Ade (**III**) adducts decompose to generate major fragment ions of *m*/*z* 419 $(M + H - NH_3)^+$, *m*/*z* 327 $(C_{24}H_{13}NC)^{+\cdot}$, *m*/*z* 314 $(C_{24}H_{12}N)^{+\cdot}$, *m*/*z* 302 $(C_{24}H_{14})^{+\cdot}$, *m*/*z* 300 $(C_{24}H_{12})^{+\cdot}$, *m*/*z* 287 $(C_{23}H_{11})^+$, and *m*/*z* 274 $(C_{22}H_{10})^{+\cdot}$ (Figure 1A–C). The $[M + H]^+$ ions of DB[*a*,*l*]P-*N*^{6}Ade produce not only the same series of fragment ions as did the other three isomers, but also additional ions of *m*/*z* 316 and 317, which are $ArNH^+$ and $ArNH_2^{+\cdot}$ (where Ar is the PAH group) (Figure 1D). These latter ions confirm that the attachment of DB[*a*,*l*]P is to the exocyclic nitrogen of the adenine species.

We showed previously that the most abundant fragment ion for the carbon-substituted adduct (at C-8 of guanine) is of *m*/*z* 327 $(DB[a,l]P\text{-}CN)^{+\cdot}$ [26]. Upon high-energy collisional activation, the ratio of the abundance of $PAH^{+\cdot}$ to that of $PAH\text{-}CN^{+\cdot}$ (or $PAH\text{-}NC^{+\cdot}$) for both BP-DNA [17, 27] and DB[*a*,*l*]P-DNA [26] adducts allows for differentiation of nitrogen versus carbon-substituted adducts. When the PAH is attached to N, as for the isomers described here, the most abundant

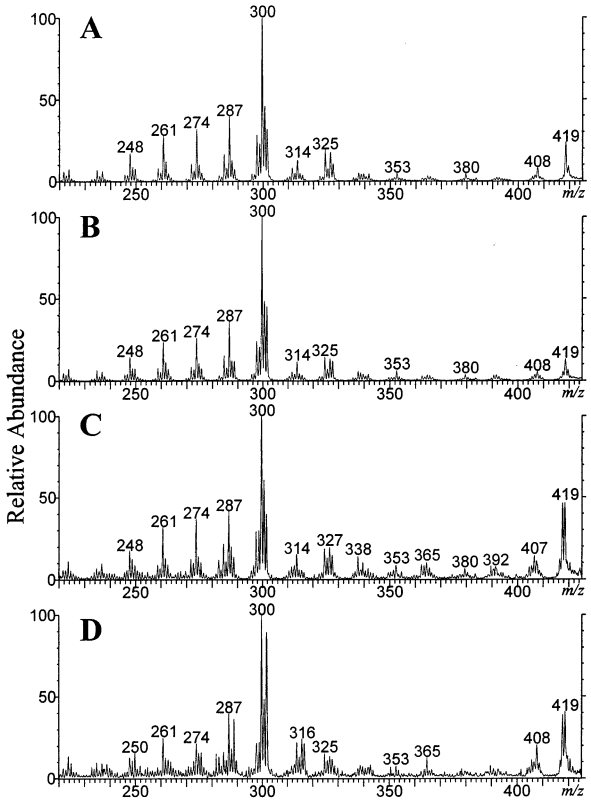

Figure 1. Partial CAD mass spectra of the $[M + H]^+$ ions from (A) DB[*a*,*l*]P-10-*N*1Ade (I), (B) DB[*a*,*l*]P-10-*N*3Ade (II), (C) DB[*a*,*l*]P-10-*N*7Ade (III), and (D) DB[*a*,*l*]P-10-N^6Ade (IV).

fragment ion is of m/z 300 $(C_{24}H_{12})^{+\cdot}$, which is formed by a hydride transfer from the DB[*a*,*l*]P moiety to the DNA base followed by heterolytic cleavage of the C–N bond between Ade and DB[*a*,*l*]P. The fragment ion of m/z 302, which is formally the DB[*a*,*l*]P radical cation, is formed by proton transfer from the adenine moiety to the DB[*a*,*l*]P, followed by heterolytic cleavage of the C–N bond between the base and DB[*a*,*l*]P. The ion of m/z 301, which is the DB[*a*,*l*]P $- H]^{+\cdot}$, results from heterolytic cleavage of the same C–N bond. The ion of m/z 287 may result from expulsion of C-10 from DB[*a*,*l*]P in the modified base, followed by the ring closure of the PAH system to form a five-membered ring. The m/z 419 ion is generated by the elimination of NH_3, presumably from the ions in which the NH_2 group is protonated (the m/z 418 ion is from matrix ions that were coselected with the precursor $[M + H]^+$).

The series of higher mass ions at m/z 392, 365, and 338 results from sequential expulsion of HCN molecules following a loss of NH_3, and the series is particularly abundant for the *N*7Ade adduct (Figure 1C). The origins of similar product ions from the six-membered ring of adenine were previously deciphered [30, 31] and may be designated as $[M + H - NH_3 - n\text{HCN}]^+$, where $n = 1$, 2, and 3, respectively. A series of fragment ions at m/z 407, 380, and 353 for *N*7Ade adduct is also produced by fragmentations of the six-membered ring of the adenine. These product ions are $[M + H - CH_2NH - n\text{HCN}]^+$, where $n = 1$ and 2, respectively. The fragmentation is also consistent with that of the BP-6-*N*7Ade adduct [17].

Table 1. Relative abundances of the fragment ions that contain the aromatic portion and of the m/z 419 ion from different DB[*a*,*l*]P-Ade adducts in high-energy CAD mass spectra

Adducts studied	$[Ar - H]^{+\cdot}$ m/z 300	Ar^+ m/z 301	$[Ar + H]^{+\cdot}$ m/z 302	m/z 419
*N*1Ade	100	47	33	24
*N*3Ade	100	48	45	14
*N*7Ade	100	60	39	46
N^6Ade	100	48	90	40

Differentiation of ring-nitrogen-substituted isomers by their CAD mass spectra is difficult, because the overall appearances of the spectra are similar. Nevertheless, comparisons of the ratios of the relative abundances of certain product ions provide evidence for distinguishing these isomers. The relative abundances of the fragment ions at m/z 300, 301, 302, and 419 are informative, and are summarized in Table 1. The relative abundance of the m/z 419 ion is the largest for the isomer in which the *N*-7 position of adenine is bonded to DB[*a*,*l*]P, whereas the relative abundance is lowest for the isomer in which *N*-3 is bonded. We suggest that formation of m/z 419 ions is promoted by protonation of NH_2 and anchimeric assistance to expel NH_3 when the NH_2 group is located on the PAH side (Scheme I). For the DB[*a*,*l*]P-10-*N*7Ade adduct, the formation of the m/z 419 ion is most competitive because a six-membered ring intermediate and tertiary carbocation are involved (Scheme IC). On the other hand, there is no obvious anchimeric assistance associated with the production of the m/z 419 ions of DB[*a*,*l*]P-10-*N*3Ade, and that ion is least abundant (Scheme ID). Another distinguishing feature is the relative abundance of the m/z 302 ion in DB[*a*,*l*]P-10-*N*3Ade, which is the largest compared to the relative abundance of m/z 302 ions from the other two isomers. Presumably, the proton attached at C-10 does not interact with other basic groups, leading to the most weakening of the C–N bond for this isomer. These abundance ratios serve as "fingerprints" of the various isomers.

Similarity Index

The calculation of a SI, which was developed as a statistical treatment to assess the similarity of two tandem mass spectra [20], may be useful for comparing spectra of closely related isomers. To evaluate the reproducibility of the HE CAD mass spectra for DB[*a*,*l*]P-10-*N*3Ade adduct, similarity indices were calculated by using eq (1), where $i - i_o$ is the difference in intensities of signals at one mass-to-charge ratio for the two spectra that are being compared and N is the number of masses used for the calculation [20]. CAD spectra of DB[*a*,*l*]P-10-*N*3Ade from consecutive acqui-

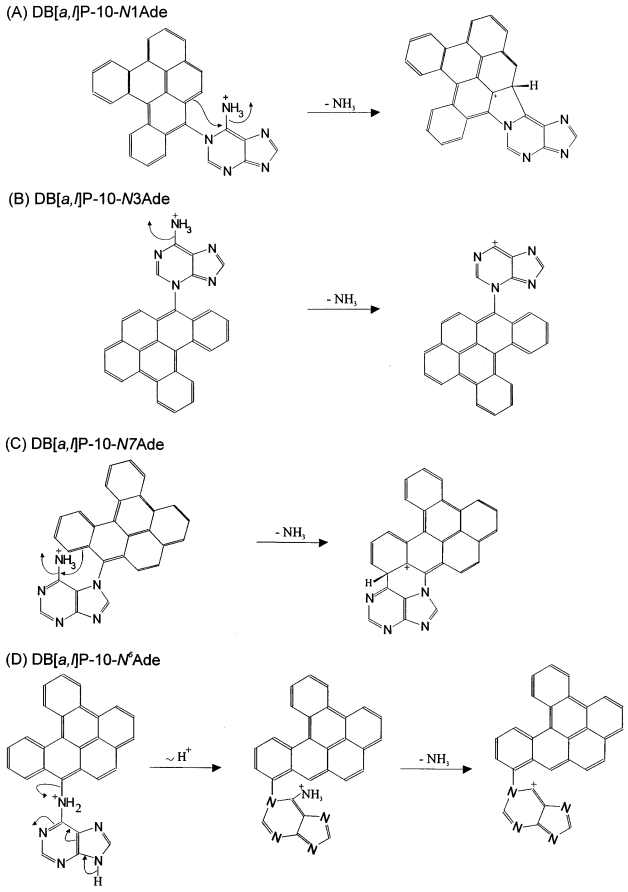

Scheme 1. Mechanism for formation of the m/z 419 ion from: (a) DB[*a*,*l*]P-10-*N*1Ade, (b) DB[*a*,*l*]P-10-*N*3Ade, (c) DB[*a*,*l*]P-10-*N*7Ade, and (d) DB[*a*,*l*]P-10-N^6Ade (other possibilities are not shown).

sitions were compared with each other for testing reproducibility over short- and long-term time periods. The resulting SI values were 17 and 18, respectively, when 14 fragment ions were used for calculation, and 17 and 19, respectively, when four ions were used in the comparison. To be able to conclude that spectra of two isomers are significantly different, the SI values obtained in a comparison should be larger than 17–19:

$$\mathrm{SI} = \sqrt{\frac{\sum [(i - i_o/i_o) \times 100]^2}{N}} \qquad (1)$$

To evaluate quantitatively the effectiveness of MS/MS for differentiating structural isomers, we calculated similarity indices by using the relative abundances of a set of fragment ions that are commonly observed for three of the four isomers that cannot be distinguished by visual observation (i.e., these isomers give qualitatively identical product-ion spectra). We omitted DB[*a*,*l*]P-10-N^6Ade because its spectrum had the unique m/z 316 and 317 ions. As shown in Table 2, the CAD mass spectrum of DB[*a*,*l*]P-10-*N*7Ade (**III**) adduct is effective for distinguishing this isomer from the other two structural isomers. On the other hand, the differences of the CAD spectra of DB[*a*,*l*]P-10-*N*1Ade (**I**) and DB[*a*,*l*]P-10-*N*3Ade (**II**) isomers do not allow for confident assignments because the SI value is only slightly larger than that acquired in the reproducibility test.

Metastable-Ion Spectra

To determine whether metastable-ion spectra are more effective for isomer distinctions, we obtained these product-ion spectra for the $[M + H]^+$ ions of the DB[*a*,*l*]P-Ade adducts (Figure 2). Although these four isomers produce fragment ions of the same mass-to-charge values that are produced upon collisional activation, the relative abundances are more distinctive for the MI spectra (see Table 3). The formation of the m/z 419 ion is the most favorable metastable-ion process for the DB[*a*,*l*]P-10-*N*7Ade adduct, whereas for DB[*a*,*l*]P-10-*N*1Ade and DB[*a*,*l*]P-10-*N*3Ade adducts, the m/z 300 ion is most readily produced. The relative abundances of the m/z 419 $[M + H - NH_3]^+$, and m/z 302 (PAH radical cation) ions in these spectra are more distinctive than are the corresponding ions in the CAD spectra. These differences clearly give information about the site of attachment of the DB[*a*,*l*]P to the adenine base. Furthermore, the m/z 316 and 317 ions in the MI mass spectrum of DB[*a*,*l*]P-N^6Ade adduct provide substantial evidence that the binding site to the DB[*a*,*l*]P moiety is the exocyclic nitrogen of adenine and allow this isomer to be easily distinguished from the other three.

We calculated SI values for the MI mass spectra by using the same sets of fragment ions as were used for the HE CAD spectra (Table 2). The SI values of MI spectra for DB[*a*,*l*]P-10-*N*3Ade (**II**) adduct from consecutive acquisitions in the short term are 20, which is essentially the same as for the HE CAD spectra. For the three isomers (I, II, and III), the SI values obtained from comparisons of MI spectra are larger than from those of CAD spectra, underscoring the conclusion the MI spectra are more effective for achieving isomer distinctions. For example, the SI value for comparison of the MI spectra of DB[*a*,*l*]P-10-*N*1Ade (**I**) and DB[*a*,*l*]P-10-*N*3Ade (**II**) adducts is 2.5 times larger than the reproducibility standard when we used 14 product ions for the calculation, whereas it is nearly the same as the standard when we compared their CAD spectra. The use of a larger number of fragment ions for a SI calculation is usually more effective than the use of a smaller number.

We were surprised to observe the extensive fragmentation that is seen in the MI spectra. It is likely that the ions at m/z 302 are primary ions, but their fragmentation to give a set of ions at m/z 300, 287, 274, 261, and 248 suggests a high internal-energy content. One possibility is that the low-mass ions in the MI spectrum are a result of CAD, owing to a collision of the precursor ion with the background gas. The magnification factors for

Table 2. Similarity index values from comparisons of the tandem mass spectra (high-energy CAD, low-energy CAD, and metastably produced product ions) of the [adduct + H]$^+$ ions of isomeric DB[*a*,*l*]P-Ade adducts

Isomers compared	HE-CAD[a]	HE-CAD[b]	Metastable[a] ion	Metastable[b] ion	LE-CAD[a]
I, II	23	22	32	52	30
I, III	27	34	36	59	39
II, III	36	38	41	34	41
II, II	19[c]/17[d]	18[c]/17[d]	20[c]	20[c]	ND[e]

[a] N = 4 (m/z 300, 302, 419, and 327).
[b] N = 14 (m/z 248, 261, 272, 274, 285, 287, 298, 299, 300, 301, 302, 325, 327, and 419).
[c] Short-term reproducibility.
[d] Long-term reproducibility.
[e] Not determined.

metastable-ion spectra (500×–1000×) compared to HECAD spectra (50×) are not consistent with this proposal. Nevertheless, we carried out a further test to confirm that the MI spectra did not contain a CAD component by examining the time dependence of metastable-ion spectra on the four-sector tandem mass spectrometer, and by using a three-sector tandem mass spectrometer (a Kratos MS-50), which has a shorter field-free region than that of the four sector. If there were collisions with background gas in the field-free region, then the spectra would become simpler as time passed and the residual collision gas was pumped away. The spectra, however, did not vary. The same series of product ions, although at different relative abundances, form in the three-sector instrument. Thus, there is no evidence for residual collisional activation in the metastable-ion experiments.

Another explanation is based on the different ionization methods. FAB produces a population of energetic ions that fragments not only to the first generation m/z 302 ions, but also to the second generation product ions. HE CAD simply increases the population of the ions in those high-energy states. Other soft ionization methods such as electrospray and MALDI, on the other hand, may produce lower-energy ions that, when activated, produce simpler spectra. To test this possibility, we produced precursor ions by ESI and activated them by HE collisions on the four-sector tandem instrument.

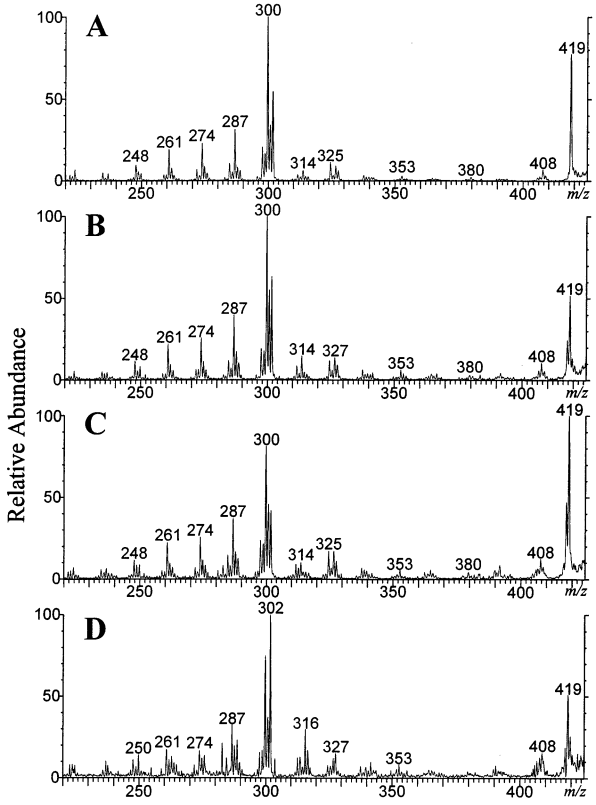

Figure 2. Partial metastable-ion mass spectra of the [M + H]$^+$ ions from (A) DB[*a*,*l*]P-10-*N*1Ade (I), (B) DB[*a*,*l*]P-10-*N*3Ade (II), (C) DB[*a*,*l*]P-10-*N*7Ade (III), and (D) DB[*a*,*l*]P-10-*N*^{6}Ade (IV).

High-Energy CAD of ESI-Produced Ions

High-energy collisional activation of the [M + H]$^+$ ions produced considerably simpler spectra for the four ESI-produced DB[*a*,*l*]P-Ade adducts. We were unable to observe metastable-ion decompositions, and most of the ions of $m/z < 300$ were not detectable upon collisional activation. For DB[*a*,*l*]P-*N*1Ade, the spectrum was simplest (Figure 3A), whereas that of DB[*a*,*l*]P-*N*3Ade shows a small but readily detectable fragmentation to the m/z 392 ion (by loss of NH_3 and HCN), as would be expected if the *N*-1 position were not substituted (spectrum not shown). This trend is accentuated for the *N*-7 isomer for which we see a considerably more abundant m/z 392 (30% relative abundance compared to 10% for *N*-1) and the appearance of an m/z 365 ion [formed by loss of NH_3 and two

Table 3. Relative abundances in metastable-ion mass spectra of fragment ions that contain the aromatic portion and of the m/z 419 ion from different DB[*a*,*l*]P-Ade adducts

Adducts studied	[Ar − H]$^{+\cdot}$ m/z 300	Ar$^+$ m/z 301	[Ar + H]$^{+\cdot}$ m/z 302	m/z 419
*N*1Ade	100	35	55	78
*N*3Ade	100	56	64	52
*N*7Ade	82	47	42	100
N^{6}Ade	76	37	100	51

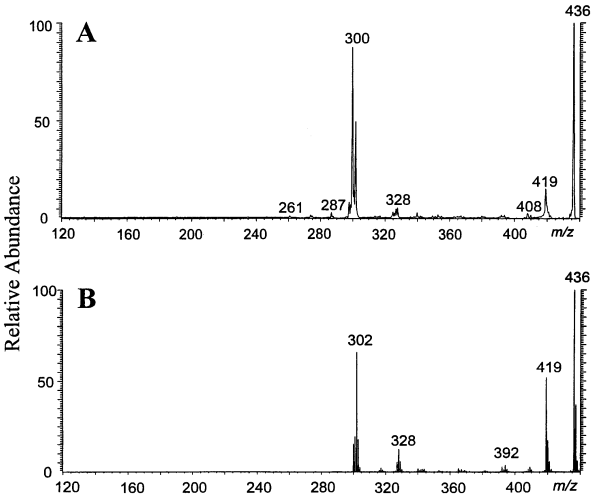

Figure 3. CAD spectra of ESI-produced $[M + H]^+$ ions from the DB[*a*,*l*]P-10-*N*1Ade (I) adduct obtained using (A) HE CAD and (B) ESI-source CAD.

molecules of HCN (spectrum not shown)]. The characteristic *m*/*z* 317 forms from the activated N^6 adduct and readily distinguishes it from the other three isomers. These observations prove that FAB-produced ions have more internal energy than those from ESI, and it is this additional energy that is responsible for the extensive fragmentation of the FAB-produced ions under metastable-ion and HE CAD conditions. Although the HE CAD spectra of electrosprayed modified bases are simpler than of those introduced by FAB, the sensitivity is considerably poorer because they are difficult to activate owing to their low internal energy.

Low-Energy CAD

Another approach to obtain product-ion spectra in MS/MS is low-energy collisional activation on triple quadrupole instruments. We were able to obtain these spectra on three commercial instruments as a function of collision energy in demonstration/application laboratories of the three manufacturers. We expected LE CAD spectra to be less information rich, but this expectation turned out to be incorrect.

The peak intensities of selected fragment ions for DB[*a*,*l*]P-10-*N*1Ade adduct at various collision-cell potentials ranging from 10 to 100 V give information on the dependence of fragmentation patterns on the internal energy of the precursor ions. By systematically changing the collision-cell potential, we obtained an energy-dependent breakdown curve (sometimes called an energy-resolved spectrum [32, 33]) for four fragment ions from the DB[*a*,*l*]P-*N*1Ade adduct (Figure 4). No detectable fragmentation occurs below 35 V. Three low-energy fragmentations produce the first-generation product ions, which are those of *m*/*z* 419, 328, and 302 at collision-cell potentials in the range of 55–60 V. The production of the *m*/*z* 300 ions is a higher-energy process (a 90-V cell potential is needed to obtain the

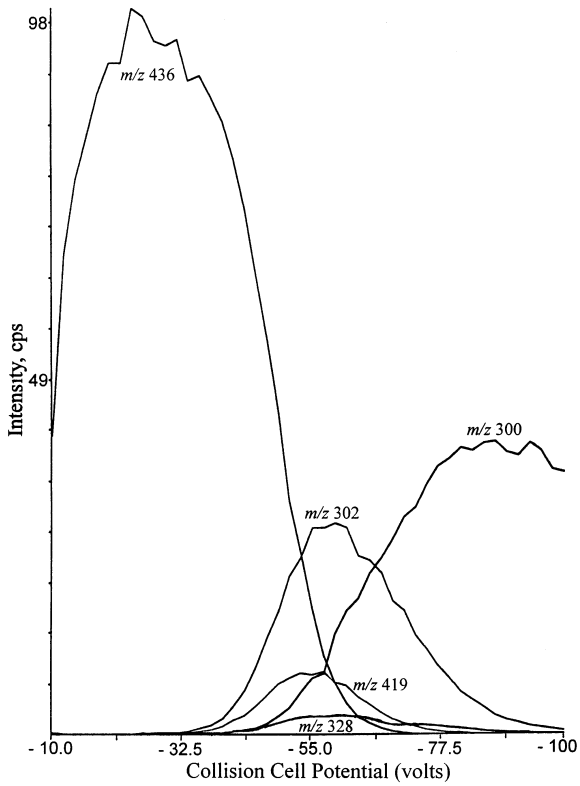

Figure 4. Energy-dependent breakdown of the $[M + H]^+$ ions (*m*/*z* 436) of the DB[*a*,*l*]P-10-*N*1Ade (I) adduct obtained from low-energy collision-induced dissociation product-ion spectra acquired by using the Sciex API 300 triple quadrupole instrument.

maximum abundance of the *m*/*z* 300 ion). The appearance of the breakdown curves indicates that this ion is a second-generation product. A collision-cell potential of 55 eV was then chosen to acquire the LE CAD mass spectra for comparison of DB[*a*,*l*]P-Ade isomers because all fragment ions are formed at this potential.

We carried out the LE CAD experiments at 55 V of collision-cell potential for the $[M + H]^+$ ions of isomeric DB[*a*,*l*]P-Ade adducts on three instruments, but we report only the spectra from the Sciex triple quadrupole. The most favorable fragmentation process for DB[*a*,*l*]P-Ade adducts under low-energy CA conditions is the formation of the *m*/*z* 302 ion, which is the PAH radical cation (Figures 4 and 5). In the low-energy CAD spectra, we see no detectable fragment ions that result from expulsion of small C_xH_y species from the PAH moiety (compare the spectral regions below *m*/*z* 300 in Figures 1 and 5), just as we observed in the HE CAD spectra of electrosprayed ions.

The formation of the *m*/*z* 317 ion from the DB[*a*,*l*]P-N^6Ade adduct occurs not only in HE CA and MI decompositions, but also in LE CAD (Figures 1D and 5D). This fragment is distinctive of this isomer and confirms that the site of DB[*a*,*l*]P attachment is the exocyclic nitrogen of adenine. The dominant series of *m*/*z* 419, 392, and 365 fragment ions, which are formed

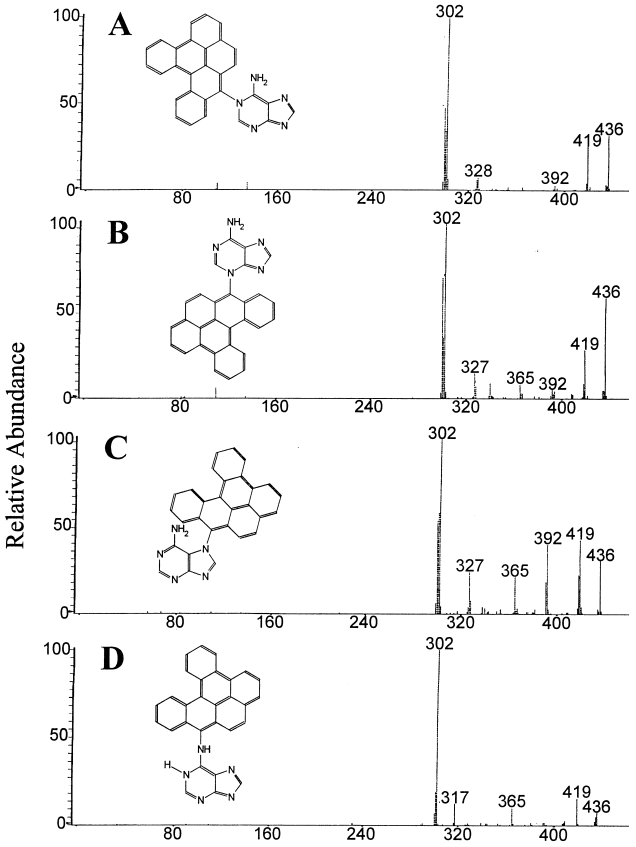

Figure 5. The low-energy CAD mass spectra of the $[M + H]^+$ ions from (A) DB[*a*,*l*]P-10-*N*1Ade (I), (B) DB[*a*,*l*]P-10-*N*3Ade (II), (C) DB[*a*,*l*]P-10-*N*7Ade (III), and (D) DB[*a*,*l*]P-10-N^6Ade (IV).

by the loss of NH_3, followed by one and two losses of HCN from the six-membered purine ring, identifies the DB[*a*,*l*]P-*N*7Ade adduct and distinguishes it from the other two ring-nitrogen-substituted isomers. The series is less abundant for the DB[*a*,*l*]P-*N*3Ade adduct, whereas it is barely detectable for the DB[*a*,*l*]P-*N*1Ade adduct. The relative abundances for loss of NH_3 (to give the m/z 419 ion) follow the same pattern as seen in the MI and HE CAD spectra of FAB-produced ions and in the HE CAD of ESI-produced ions, but the trend is not as dramatic in the LE CAD spectra (compare Figures 1, 2, and 5).

For low-energy collisionally induced fragments of the DB[*a*,*l*]P-Ade isomers, the abundances of four fragment ions, which are part of the same set used in HE CAD and metastable-ion analysis, were used to calculate SI values and quantify the differences of the LE CAD mass spectra (see the last column in Table 2). We did not carry out consecutive acquisitions for testing the reproducibility of LE CAD experiments because we did not see the prospect of calculating SI values at the time of visiting the vendors' laboratories. Nevertheless, the SI values for distinguishing the four isomers are comparable or larger than those from HE CAD and show that LE CAD spectra are as or more effective than HE CAD spectra for distinguishing positional isomers.

Table 4. Similarity index values of the LE-CAD mass spectra of DB[*a*,*l*]P-10-*N*1Ade adduct obtained from three different instruments

	Sciex	Finnigan	Micromass
Sciex		55	23
Finnigan			23

The LE CAD experiments for DB[*a*,*l*]P-Ade adducts were also carried out on triple quadrupole instruments manufactured by Finnigan and Micromass. Because the low-energy CAD method is sensitive to collision energy, the nature of collision gas, and the pressure of collision gas, changes in one of these parameters may affect the energy deposition in the selected-precursor ions and, consequently, their fragmentation patterns. As a result, we expected the spectra to be reproducible on one instrument, but not from instrument to instrument. The selected-parent ions decompose to produce the same product ions observed in the CAD spectra acquired with the Sciex instrument. The spectra from instrument to instrument are reproducible, as can be seen by using the SI to make comparisons (Table 4), and they attest to the utility of low-energy CAD on triple quadrupole instruments for distinguishing isomers.

ESI-Source CAD

Another method for obtaining structural information is ESI-source CAD; here CAD is induced by accelerating the ions in the high-pressure region of the electrospray source. Although this method lacks the capability of precursor-ion selection and, therefore, is susceptible to the presence of impurities, ESI-source CAD on magnetic sector mass spectrometers benefits from their high mass resolving power. ESI-source CAD spectra of the four DB[*a*,*l*]P adducts show formation of the m/z 302 (PAH radical cation) as the dominant fragment, whereas HE CAD produces a most abundant m/z 300 ($C_{24}H_{12}^+$) (see Figure 3B for a typical example). In addition, observation of higher abundance of the m/z 317 fragment ion in the ESI-source CAD of the DB[*a*,*l*]P-N^6Ade adduct distinguishes this adduct from the other three isomers. Another interesting observation is that fragment ions due to dissociation of the PAH moiety are absent in ESI-source CAD of all four DB[*a*,*l*]P adducts. The ESI-source CAD spectra of DB[*a*,*l*]P adducts more closely match the LE CAD than the HE CAD spectra.

MALDI PSD

Product ion spectra obtained via MALDI-PSD are also information rich (see Figure 6). The ion chemistry associated with PSD of the selected precursor ions is qualitatively identical to that underlying LE CAD. There are no fragment ions below m/z 300, the ion of m/z 302 is always the most abundant, and the trend for

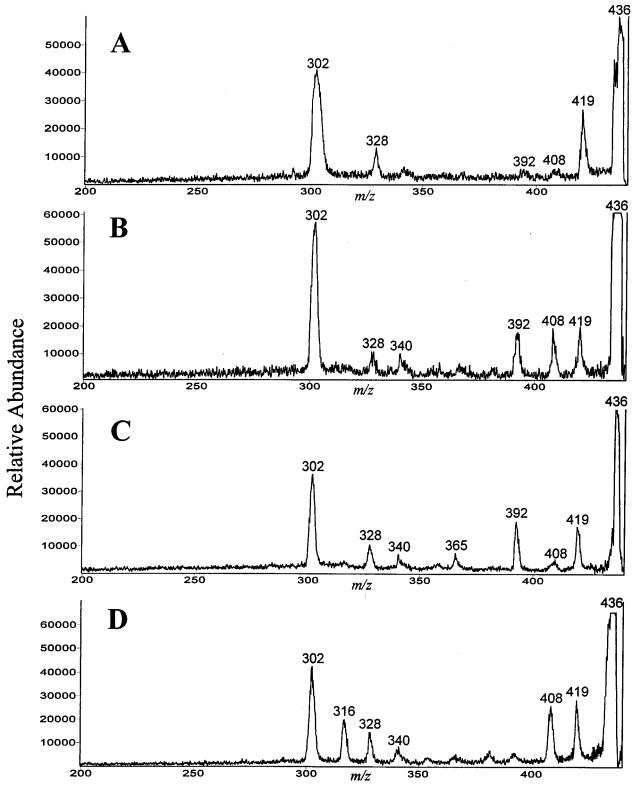

Figure 6. MALDI-PSD spectra of the $[M + H]^+$ ions from (A) DB[*a*,*l*]P-10-*N*1Ade (I), (B) DB[*a*,*l*]P-10-*N*3Ade (II), (C) DB[*a*,*l*]P-10-*N*7Ade (III), and (D) DB[*a*,*l*]P-10-N^6Ade (IV).

the m/z 419, 392, 365 series is the same as that for the LE CAD spectra. The formation of the m/z 317 ion is observed for DB[*a*,*l*]P-N^6-Ade, indicating attachment at the exocyclic amino group. The absence of this ion in the spectra of the other nitrogen substituted isomers allows for the distinction of this isomer from the others. Many of the similarities between PSD and LE CAD spectra are key for distinguishing the four isomers.

We assessed the reproducibility of these PSD spectra by using similarity indices calculated from three to five ions, depending on the isomer being studied. The largest SI value is for the DB[*a*,*l*]P-10-N^6Ade isomer: SI = 10 (long term) and SI = 6 (short term). SI values from short-term studies of DB[*a*,*l*]P-10-*N*1Ade, DB[*a*,*l*] P-10-*N*3Ade, and DB[*a*,*l*]P-10-*N*7Ade are 6, 9, and 6, respectively. We made interspectral comparisons for the DB[*a*,*l*]P-10-*N*3Ade and DB[*a*,*l*]P-10-*N*7Ade isomers (abundances of four ions at m/z 328, 392, 408, and 419 were used) and obtained a SI value of 33. The DB[*a*,*l*]P-10-N^6Ade and DB[*a*,*l*]P-10-*N*1Ade isomers are easily distinguished from the others owing to the formation of distinctive ions for the former and the absence of them for the latter.

Conclusion

One goal of our research is to use tandem mass spectrometry to determine the structure of modified DNA bases, nucleosides and nucleotides, that are isolated from in vitro and in vivo experiments. A necessary step in achieving this goal is to establish that the fragmentation chemistry occurring in tandem mass spectrometry is sufficiently distinctive to determine the structure of modified DNA materials. The biggest challenge is to determine the structure of closely related isomers, and this challenge provided the motivation for the study of the four *N*-substituted DB[*a*,*l*]P isomers. These isomers should be easily distinguished from a fifth isomer, DB[*a*,*l*]P-10-C8Ade, on the basis of earlier work with guanine isomers [26].

Five commonly used MS/MS methods (i.e., HE CAD, MID, LE CAD, ESI-source CAD, and PSD) are able to distinguish easily three isomers and sometimes all four. The methods of activation are comparably effective, but the basis for making distinctions is different in HE and LE CAD. For HE CAD, we find more distinctiveness in the relative abundances for the ions of m/z 300, 302, and 419 (the latter produced by loss of NH_3), whereas in LE CAD and PSD, the greater differences stem from the lose of one and two HCNs, following the loss of NH_3, to give the ions of m/z 392 and 365. The activation methods allow identification of the modified exocyclic NH_2 group from the production of the m/z 317 ion. The close similarity of PSD and LE CAD spectra, which was also seen for peptides, suggests a mechanistic link between the two processes [19b, c]. The spectral differences have a basis that can be understood in terms of ion chemistry, thus opening the door to interpret spectra of materials for which no reference compounds are yet available. The choice of method for these compounds depends on sensitivity, not specificity, and the advantage now is with LE CAD of ESI-produced ions and PSD of MALDI-produced ions.

Acknowledgments

This research was supported by the National Institutes of Health grant no. 1P01CA49210 and grant no. 2P41RR00954. The authors thank scientists at Finnigan, Micromass, and Sciex for assisting with data acquisition by triple-quadrupole mass spectrometry.

References

1. Irving, C. C. In *Methods in Cancer Research*; Busch, H., Ed.; Academic: New York, 1973; Vol. 7, pp 189–244.
2. Glover, P. L., Ed., In *Chemical Carcinogens and DNA*; Chemical Rubber Company: Boca Raton, FL, 1979; Vols 1 and 2.
3. Miller, J. A. *Cancer Res.* **1970,** *30*, 559–576.
4. Miller, E. C.; Miller, J. A. *Cancer* **1981,** *47*, 2327–2345.
5. Cavalieri, E. L.; Rogan, E. G. In *Free Radicals in Biology*; Pryor, W. A., Ed.; Academic: New York, 1984; Vol VI, pp 323–369.
6. Cavalieri, E. L.; Rogan, E. G. *Environ. Health Perspect.* **1985,** *64*, 69–84.
7. Cavalieri, E. L.; Rogan, E. G. *Pharmac. Ther.* **1992,** *55*, 183–199.
8. Sims, P.; Grover, P. L. In *Polycyclic Hydrocarbons and Cancer*; Gelboin, H. V.; Ts'o, P. O. P., Eds.; Academic: New York, 1981; Vol 3, pp 117–181.

9. Conney, A. H. *Cancer Res.* **1982,** *42*, 4875–4917.
10. Jankowiak, R.; Small, G. J. *Anal. Chem.* **1989,** *61*, 1023A–1032A.
11. Vahakangas, K.; Trivers, G.; Rowe, M.; Harris, C. C. *Environ. Health Perspect.* **1985,** *62*, 101–104.
12. Gupta, R. C.; Reddy, M. V.; Randerath, K. *Carcinogenesis* **1982,** *3*, 1081–1092.
13. Randerath, K.; Reddy, M. V.; Gupta, R. C. *Proc. Natl. Acad. Sci. USA* **1981,** *78*, 6126–6129.
14. Roberts, D. W.; Benson, R. W.; Groopman, J. D.; Flammang, T. J.; Nagle, W. A.; Moss, A. J.; Kadlubar, F. F. *Cancer Res.* **1988,** *48*, 6336–6342.
15. Harris, C. C.; Yolken, R. H.; Hsu, I. C. *Methods Cancer Res.* **1982,** *20*, 213–243.
16. RamaKrishna, N. V. S.; Cavalieri, E. L.; Rogan, E. G.; Dolnikowski, G. G.; Cerny, R. L.; Gross, M. L.; Jeong, H.; Jankowiak, R.; Small, G. J. *J. Am. Chem. Soc.* **1992,** *114*, 1863–1874.
17. RamaKrishna, N. V. S.; Gao, F.; Padmavathi, N. S.; Cavalieri, E. L.; Rogan, E. G.; Cerny, R. L.; Gross, M. L. *Chem. Res. Toxicol.* **1992,** *5*, 293–302.
18. Wellemans, J.; Cerny, R. L.; Gross, M. L. *Analyst* **1994,** *119*, 497–503.
19. (a) Spengler, B.; Kirsch, D.; Kaufmann, R. *J. Phys. Chem.* **1992,** *96*, 9678–9684; (b) Kaufmann, R.; Kirsch, D.; Spengler, B. *Int. J. Mass Spectrom. Ion Processes* **1994,** *131*, 355–385; (c) Medzihradszky, K. F.; Adams, G. W.; Burlingame, A. L.; Bateman, R. H.; Green, M. R. *J. Am. Soc. Mass Spectrom* **1996,** *7*, 1–10.
20. Lay, J. O., Jr.; Gross, M. L.; Zwinselman, J. J.; Nibbering, N. M. M. *Org. Mass Spectrom.* **1983,** *18*, 16–21.
21. Rindgen, D.; Turesky, R. J.; Vouros, P. *Chem. Res. Toxicol.* **1995,** *8*, 1005.
22. Kowalski, E. M.; Chaudhary, A. K.; Blair, I. A. *Proceedings of the 43rd ASMS Conference on Mass Spectrometry and Allied Topics*; Atlanta, GA, May 21–26, 1995; p 589.
23. Rindgen, D.; Turesky, R. J.; Vouros, P. *Proceedings of the 43rd ASMS Conference on Mass Spectrometry and Allied Topics*; Atlanta, GA, May 21–26, 1995; p 590.
24. Yen, T.-Y.; Christova-Gueorguieva, N. I.; Scheller, N.; Swenberg, J. A.; Charles, M. J. *Proceedings of the 43rd ASMS Conference on Mass Spectrometry and Allied Topics*; Atlanta, GA, May 21–26, 1995; p 497.
25. Li, K. L.; Byun, J.; Gross, M. L.; Yen, T.-Y.; Jankowiak, R.; Zawzow, D.; Small, G. J.; Rogan, E. G.; Cavalieri, E. L., unpublished.
26. RamaKrishna, N. V. S.; Padmavathi, N. S.; Cavalieri, E. L.; Rogan, E. G.; Cerny, R. L.; Gross, M. L. *Chem. Res. Toxicol.* **1993,** *6*, 554.
27. Rogan, E.; Cavalieri, E.; Tibbels, S.; Cremonesi, P.; Warner, C.; Nagel, D.; Tomer, K.; Cerny, R.; Gross, M. *J. Am. Chem. Soc.* **1988,** *110*, 4023–4029.
28. Gross, M. L. *Tandem Mass Spectrometry: Multisector Magnetic Instruments*. In *Methods in Enzymology, Vol. 193, Mass Spectrometry*; McCloskey, J. A., Ed.; Academic: San Diego, 1990; pp 131–153.
29. George, M.; Wellemans, J. M. Y.; Cerny, R. L.; Gross, M. L.; Li, K.; Cavalieri, E. L. *J. Am. Soc. Mass Spectrom.* **1994,** *5*, 1021–1025.
30. Crain, P. F.; McCloskey, J. A. Naturally modified nucleosides from nucleic acids. In *Biological Mass Spectrometry*; Gross, M. L., Ed.; Wiley: West Sussex, England, 1994; pp 509–537.
31. Crain, J. M.; Gregson, J. M.; McCloskey, J. A.; Nelson, C. C.; Pelfier, J. M.; Philips, D. R.; Pomerantz, S. C.; Reddy, D. M. Characterization of posttranscriptional modification in nucleic acids by tandem mass spectrometry. In *Mass Spectrometry in the Biological Science*; Burlingame, A. L.; Ed.; Humana: Totowa, NJ, 1996; pp 497–517.
32. Brodbelt, J. S.; Kenttämaa, H. I.; Cooks, R. G. *Org. Mass Spectrom.* **1988,** *23*, 6–9.
33. Horning, J. M.; Wood, J. M.; Gord, J. R.; Freiser, B. S.; Cooks, R. G. *Int. J. Mass Spectrom. Ion Processes* **1990,** *101*, 219–243.